

Application of Fast Response Dual-Colour Pyroelectric Detectors with Integrated Op Amp in a Low Power NDIR Gas Monitor

InfraTec GmbH, Gostritzer Str. 61-63, 01217 Dresden

1. Introduction

Monitoring the concentration of carbon dioxide (CO₂) is increasingly being used as a surrogate for determining indoor air quality (IAQ) and to decrease energy consumption of enclosed office spaces. Currently available CO₂ sensors for these applications, however, are not being used in private homes since residential units would have to be easier to handle, maintenance free, lower cost and require lower power consumption. Over the long term (e.g., 5 years) residential units based on Non-Dispersive Infrared (NDIR) must be able to make accurate and repeatable measurements to a postulated accuracy of 100 ppm over a total range of 0 ppm to 2000 ppm /1/.

Currently available IAQ / CO₂ sensors based on pyroelectric detectors that are sensitive to a change in IR radiation, typically contain a miniature incandescent lamp as the IR source. The IR source is usually electrically modulated at an optimal frequency for source efficiency and pyroelectric detector sensitivity / performance. Since the power consumption of the incandescent lamp is very high, this design configuration is not practical for battery or bus powered applications that would make up a large portion of residential market monitors.

The total power consumption of the sensor required operating the IR source and the sensor analog electronics must be reduced.

2. Solution

To address the problems associated with residential CO₂ monitors, a new sensor has been developed /2/. A single pulse of IR source radiation will generate a pyroelectric detector signal. Source power consumption can be reduced by an order of magnitude by operating the source with pulse duration of several 100 ms and pauses of several seconds. In order to achieve reliable measurements, a new detector design was developed to provide the maximum signal amplitude for the anticipated modulation frequencies. This new detector runs in current mode with an integrated Op Amp as transimpedance amplifier. Fig. 1 shows the schematics of a common voltage mode detector and a current mode detector.

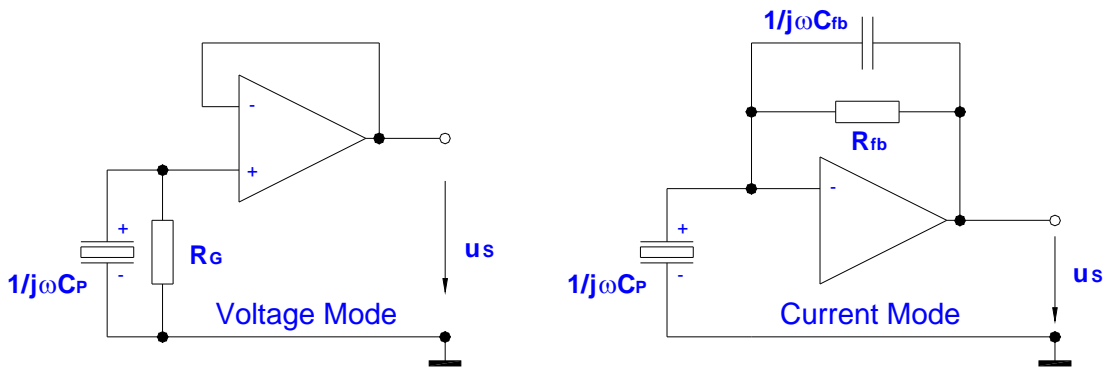


Fig. 1: Principal schematic of voltage mode and current mode pyroelectric detectors

Modern low power Op Amps with low current i_{ni} and voltage noise e_{ni} ensure the same signal to noise ratio as in a simple JFET source follower, however due to the considerably lower electrical time τ_E constant it allows a considerably higher responsivity, described by equation (1)-(3) /3/.

$$R_V = \frac{\tilde{u}_S}{\tilde{\Phi}_S} = \frac{\alpha \tau_F}{G_T} \omega p A_S R_{G/fb} \frac{1}{\sqrt{1 + (\omega \tau_T)^2}} \frac{1}{\sqrt{1 + (\omega \tau_E)^2}} \quad (1)$$

$$\tau_{EVM} = C_P R_G \quad \text{for the voltage mode and} \quad (2)$$

$$\tau_{ECM} = C_{fb} R_{fb} \quad \text{for the current mode} \quad (3)$$

with the signal voltage u_S , the incident radiation flux Φ_S , the absorption coefficient α of the pyroelectric chip, the IR filter transmittance τ_F , the thermal conductance between pyroelectric chip and its surrounding G_T , the angular frequency ω , the IR sensitive area A_S , the thermal time constant τ_T , the electrical time constant τ_E , the electrical capacity of the pyroelectric chip c'_P , the feedback capacity C_{fb} , the gate resistance R_G and the feedback resistance R_{fb}

In Figure 2, typical frequency dependence of the responsivity R_V of both modes is shown. The thermal time constant is τ_T 160 ms for both modes, but the electrical time constant τ_E differs by the factor 94.

The maximum signal was found at the frequency f_{max} :

$$f_{max} = \frac{1}{2\pi} \frac{1}{\sqrt{(\tau_T \tau_E)}} \quad (4)$$

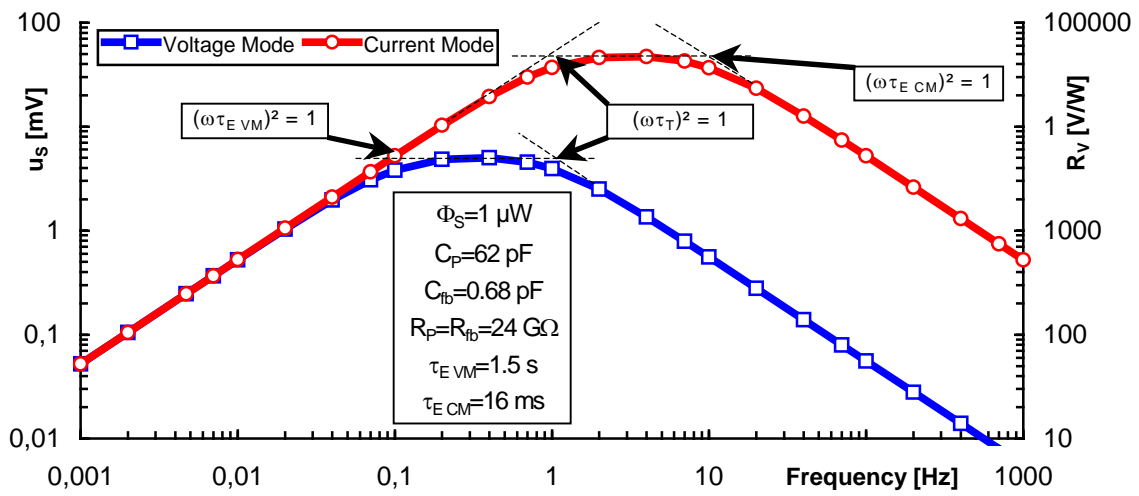


Fig. 2: Comparison of signal voltage and responsivity of voltage and current mode respectively

The step response of pyroelectric detectors in the current and voltage mode is shown in Fig. 3 and can be described by equation (5):

$$u_S(t) = \alpha \tau_W \hat{\Phi}_S R_{G/fb} \frac{p}{c'_P} \frac{1}{t_P} \left(e^{-\frac{t}{\tau_E}} - e^{-\frac{t}{\tau_T}} \right) \quad (5)$$

with the pyroelectric coefficient p , the volume specific heat capacity of the pyroelectric chip c'_P , the thickness of the pyroelectric chip t_P .

The maximum signal voltage is observed at t_{max} :

$$t_{max} = \ln \frac{\tau_T}{\tau_E} \left(\frac{1}{\tau_E} - \frac{1}{\tau_T} \right)^{-1} \quad (6)$$

The larger the ratio of τ_T / τ_E the faster the maximum signal is reached. In the current mode the time to reach the maximum signal t_{max} is lower than the thermal time constant τ_T if the electrical time constant τ_E is sufficiently small.

The advantages of the current mode are obvious:

- there is a very high responsivity ($R_V > 100,000$ V/W)
- there is a low electrical time constant and therefore a fast response.

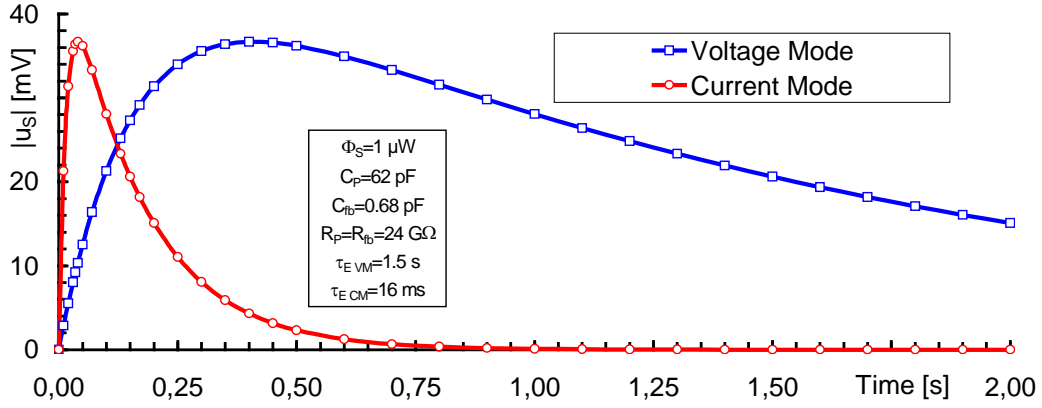


Fig. 3: Pulse response of signal voltage of voltage and current mode

Additional advantages can be obtained by the proper choice of appropriate Op Amps:

- there is a very low output offset together with a very low offset temperature drift
- there is very low current noise together with a lower temperature drift of the specific detectivity at low frequencies ($f < 100\text{Hz}$)
- there is no signal and signal/noise-ratio loss when using the parallel compensation in thermal compensated detectors
- there is a very low power consumption and therefore a short warm-up phase and fast recovery time

3. Detector

In order to guarantee optimum operation in the current and voltage mode, the detectors shall be built with:

- thermal time constant τ_T : $\tau_T \geq 150\text{ ms}$
- electrical time constant τ_E : $\tau_E \leq \tau_T / 10$ ($10\text{ G}\Omega \leq R_{fb} \leq 100\text{ G}\Omega$, $C_{fb} \ll 1\text{ pF}$)

The choice of the OpAmp is based on the following criteria:

- low power, low voltage
- low current noise i_{ni} , low voltage noise e_{ni}
- high input resistance R_i , low input capacitance C_i
- low offset voltage
- high Gain-Bandwidth Product GBW
- size, price, delivery terms

CMOS based Op Amps have been found to meet the above criteria best. Compared to Op Amps with JFET input stage they show lower input current noise and they are available as low power / low voltage types.

Due to the capacitive impact of the pyroelectric chip at the input of the transimpedance-amplifier a feedback capacitance C_{fb} is required to assure stability. The use of a minimal capacitance C_{fb} according to equation (7) will ensure that the signal bandwidth will not be limited too much. /4/:

$$C_{fb} = \sqrt{\frac{C_P + C_i}{GBW R_{fb}}} \quad (7)$$

The capacitance at the negative Op Amp input will result in the so-called noise gain phenomena /5/, since the amplification of the input noise voltage e_{ni} arises. This amplification appears with high feedback-resistors R_{fb} and high capacitance C_P of both the radiation sensitive and the thermal compensation pyroelectric chips already at relatively low frequencies.

$$\tilde{u}_{ne} \approx e_{ni} \left(1 + \frac{C_P + C_i}{C_{fb}} \right) \quad (8)$$

In order to achieve optimal detector specific detectivity, it is essential to pay particular attention to the choice of the appropriate Op Amp so as to minimize low input noise voltage e_{ni} .

As an example the dual-colour detectors LIM 162 and LIM 262 developed for low power NDIR measurement are shown in Fig. 4. The detectors are packaged in a TO5 housing. The Op Amp and the pyroelectric chips are placed on a ceramic board by adhesive joining and chip&wire technology. The feedback resistance of the LIM 162 and the LIM 262 is 24 GΩ and 100 GΩ respectively. The LIM 262 is thermal compensated with anti-parallel compensation elements at the amplifier input, which makes the detector very stable against ambient temperature drifts. The small feedback capacitance of 250 fF is realized on board by parallel strip lines. The fast response allows measurement of infrared radiation pulses as short as 50 ms.

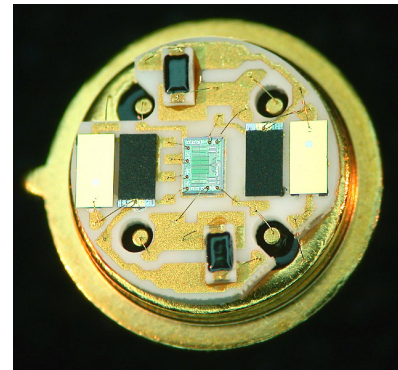


Fig 4: TO5 detector header of the detectors LIM 162/262

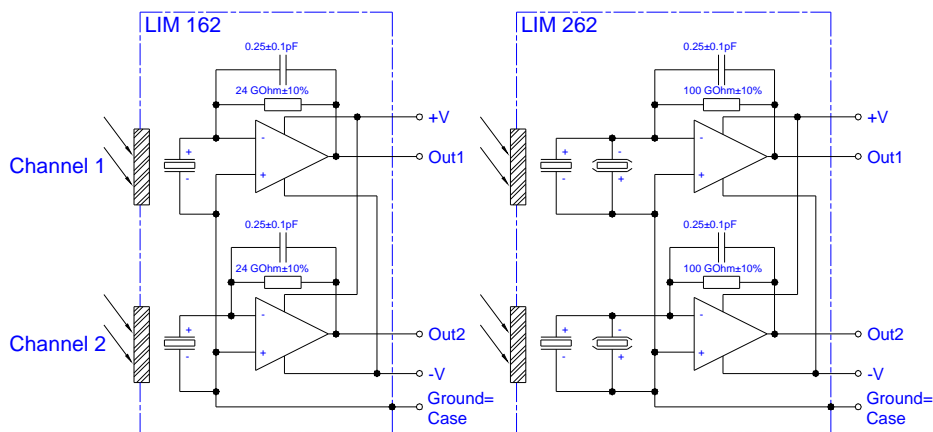


Fig 5: Schematic of the detectors LIM 162/262

The frequency dependence of the responsivity and specific detectivity are shown in fig. 6. In the frequency range of (1...10) Hz, mostly used in NDIR gas analysers the maximum of responsivity and specific detectivity could be observed as high as 40/115 kV/W and $3/5 \cdot 10^8$ cmHz^{1/2}/W.

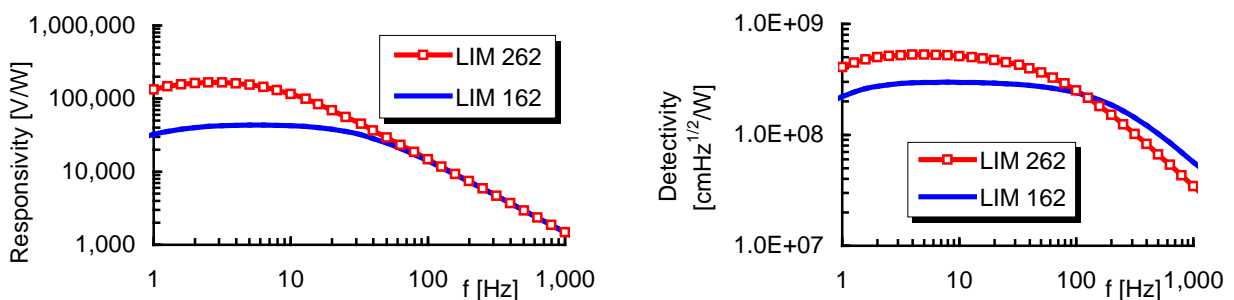


Fig 6: Frequency dependence of responsivity and specific detectivity of LIM 162 and LIM 262 /6/

4. Gas Monitor

In order to demonstrate the advantages of the new detector concept, the LIM 262 was used in a low power CO₂ gas monitor. The configuration and the block diagram are shown in Fig. 7 and 8. A gold plated gas cell (slitted tube) was used that has an absorption path length of 5 cm. A miniature incandescent lamp was used as the IR source and installed at one end of the gas cell. The LIM 262 pyroelectric detector was installed at the other end. Due to the high signal of approximately 1 V and the low offset of 1 mV substantial reduction in the complexity of the analog circuit is achieved. The micro-controller MSP430 is used for the conversion and the processing of the signals. It features very low current consumption and 12 bit resolution /7/.

In the units designed for the pulse mode both step responses at switch on and switch off of the IR source was chosen to obtain the maximum signal as shown in Fig 9. Including the 2nd pulse response, which occurs at

switch off of the lamp, the turn-on-time increases, but the sensitivity is considerably improved. Fig. 11 shows the detector signal of a unit powered in chopper mode. The maximum signal amplitude in the chopper mode is comparable to the amplitude in the pulse mode. This enables the use of the same hardware for a range of modulation frequencies as shown in Fig. 12. The CO₂ sensitivity, shown in fig. 10 and 12 at 2000 ppm in pulse and in chopper mode is 95 $\mu\text{V}/\text{ppm}$ at 0.5 s pulse duration and 75 $\mu\text{V}/\text{ppm}$ at 1.5 Hz modulation frequency. The newly developed pulse mode does not achieve the same signal-to-noise-ratio or accuracy as the common chopping mode. Therefore, a smart measurement algorithm [8] alternates between the two modes and recalibrates the pulse mode from time to time as represented in Fig. 13.

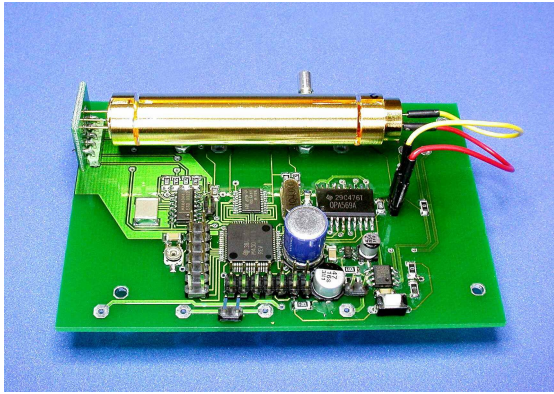


Fig. 7: Prototype of the low power CO₂ gas monitor

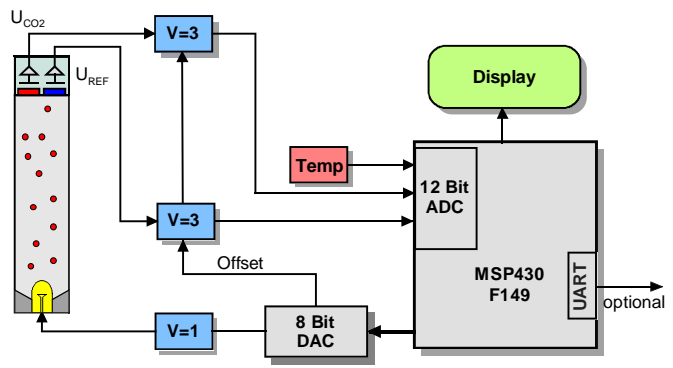


Fig. 8: Block diagram of the CO₂ gas monitor

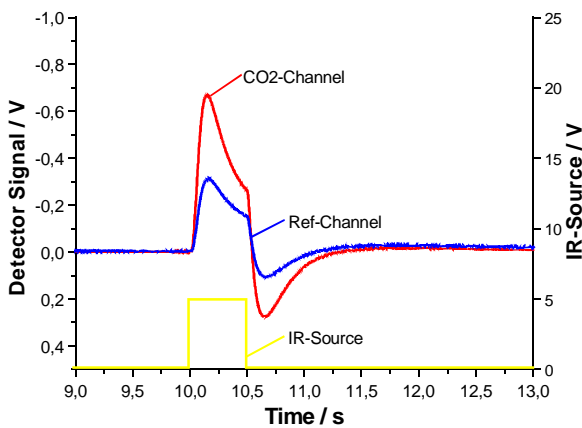


Fig. 9: Detector response in pulse mode

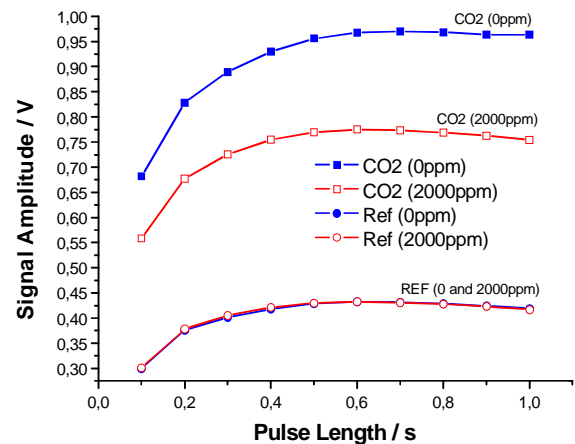


Fig. 10: Dependence of the signal from the pulse duration

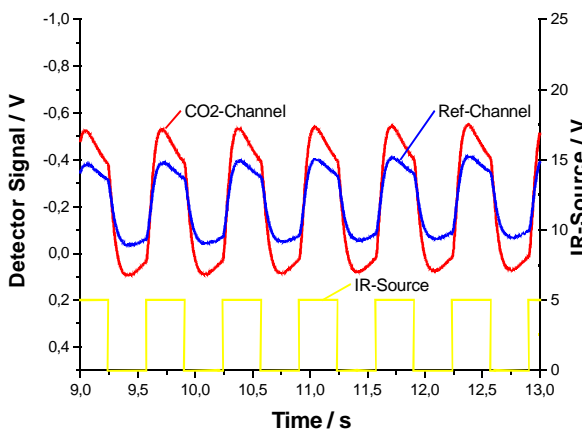


Fig. 11: Detector response in chopper mode

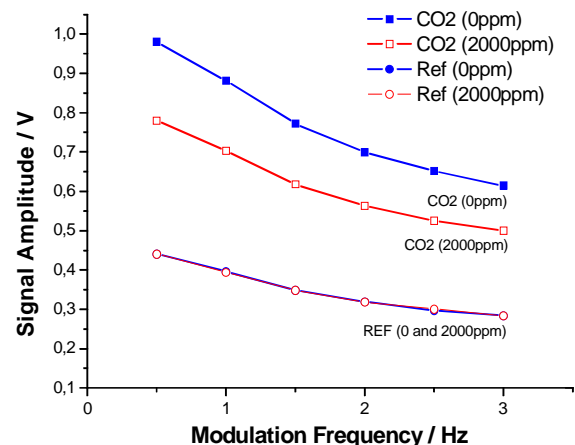


Fig. 12: Dependence of the signal from the chopper frequency

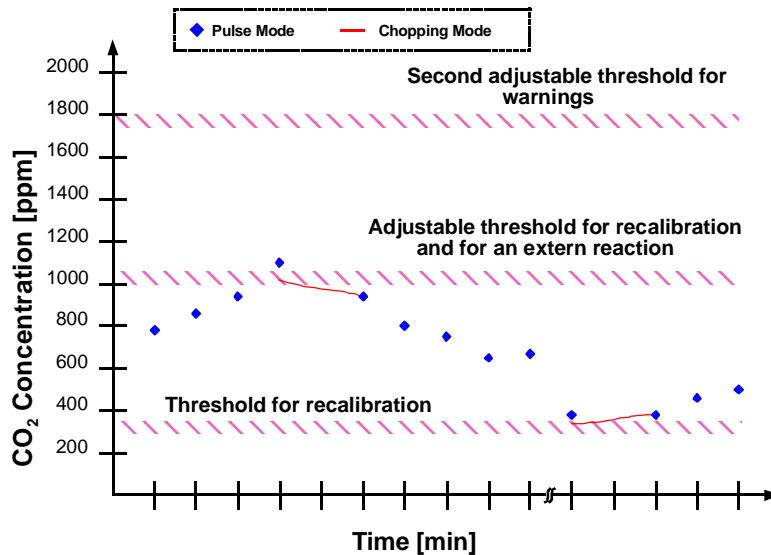


Fig. 13: Measurement algorithm with pulse and chopping mode

In chopping mode the system consumes up to 300 mW. If one cycle is measuring in pulse mode for 23.5 hours and measuring in chopping mode for 30 minutes, the average power consumption of this cycle is 8.2 mW.

The results have been achieved in the Project "ECOS" which was sponsored by the "Deutsche Bundesstiftung Umwelt (DBU)".

5. References

- /1/ J. Staab
„Industrielle Gasanalyse“
R. Oldenburg Verlag München Wien, 1994
- /2/ M. Gürtner, N. Neumann, F. Schneider,
„NDIR Gas measurement with an Actice Multicolor Detector and Pulse Response Evaluation for Low Power Applications“
AMA Fachtagung Sensor 2003, Nürnberg Juni 2003
- /3/ G. Hofmann, N. Neumann
„Spannungs- und Strombetrieb pyroelektrischer Sensoren“
Experimentelle technik der Physik 29(1981) 3, 267-272
- /4/ R. A. Pease
“What’s all this transimpedance amplifier stuff, anyhow?”
<http://www.elecdesign.com/Globals/PlanetEE/Content/13934.html>
- /5/ J. Graeme
„Photo Diode Amplifiers: Op Amp Solutions“
Mc Graw Hill, 1995
- /6/ Datenblatt LIM 162/262,
InfraTec GmbH, <http://infratec.de/sensorik/pdf/lim262.PDF>
- /7/ Product folder MSP430 F149
Texas Instruments Inc., <http://focus.ti.com/docs/prod/folders/print/msp430f1491.html>
- /8/ N. Neumann, G. Gürtner, M. Heinze; F. Schneider
„Verfahren und NDIR-Gasanalysator zur Bestimmung der Konzentration von Gasen Dämpfen“
Offenlegungsschrift DE 102 21 708 A1